3B.7

PHYSICAL MECHANISMS CONTROLLING SELF-AGGREGATION OF CONVECTION IN IDEALIZED NUMERICAL MODELING SIMULATIONS

Allison A. Wing* and Kerry A. Emanuel
Program in Atmospheres, Oceans, and Climate, Massachusetts Institute of Technology, Cambridge, MA

1. INTRODUCTION

Moist convection in the tropical atmosphere is often organized into clusters containing many individual convective cells. The value of understanding how convection organizes cannot be overstated. Clusters of organized convection are ubiquitous in the tropics (e.g., Machado and Rossow, 1993; Mapes and Houze Jr., 1993) and have important impacts on weather and climate. They are responsible for much of the rainfall and cloudiness over the tropics, with approximately 50% of tropical rainfall due to mesoscale convective systems (Nesbitt et al., 2000). This allows tropical cloud clusters to modulate the radiative heating of the surface and atmosphere and influence the large-scale circulation and moisture distribution. In idealized modeling studies (e.g., Bretherton et al., 2005) and observations (Tobin et al., 2012, 2013), there is a systematic dependence of mean humidity and radiative fluxes on the degree of convective aggregation. Therefore, understanding how and why tropical convection organizes is important for understanding both tropical and global climate variability, and climate sensitivity. Globally, 6.4% of tropical cloud clusters evolve into tropical cyclones each year (Hennon et al., 2011), so tropical convective organization is also tightly linked to the problem of tropical cyclogenesis. Finally, understanding the mechanisms by which convection organizes may lead to insights on the Madden-Julian Oscillation, which can be considered convective organization on a large scale. The MJO has a direct impact on weather in the Indian and western Pacific Oceans and modulates tropical cyclone activity, yet, a complete theory for its existence and propagation characteristics remains elusive.

In this study, the fundamental mechanism underlying the self-aggregation of convection is explored using a cloud-resolving model. The objective is to identify and quantify the interactions between the environment and the convection that allow the convection to spontaneously organize into a single cluster. This study addresses several questions:

- How does self-aggregation evolve?
- Which feedbacks are important and what are their magnitudes?
- What physical mechanisms are behind the feedbacks controlling self-aggregation?

2. MODEL SIMULATIONS

The model used is the System for Atmospheric Modeling, henceforth referred to as SAM (Khairoutdinov and Randall, 2003). SAM is a three-dimensional cloud resolving model that employs the anelastic equations of motion. The prognostic thermodynamics variables are the total nonprecipitating water, total precipitating water, and the liquid water/ice static energy. The simulations discussed here were performed with a domain size of 768 x 768 km^2 with 64 vertical levels and rigid lid at 28 km. The horizontal resolution was 3 km, and doubly periodic lateral boundary conditions were employed. The model was initialized with a sounding from the domain average of a smaller domain run in radiative-convective equilibrium with white noise added in the boundary layer temperature field. There is no mean wind or other external forcing imposed. We used a fully interactive radiation scheme (RRTM), with solar insolation constant and equal to a value of 413.98 W/m^2 and no diurnal cycle. The surface sensible and latent heat fluxes were computed interactively. Finally, we performed simulations at fixed sea surface temperature (SST), with values between 295K and 312K, but most of the results shown here are for the simulation at 305 K.

3. EVOLUTION OF SELF-AGGREGATION

Simulations of convection in radiative-convective equilibrium using three-dimensional cloud system resolving models often produce distributions of convection that are nearly random in space and in time. Figure 1a shows an example of this with a snapshot of

**Corresponding author address:* Allison A. Wing, Massachusetts Institute of Technology 54-1815, Cambridge, MA 02139; email: awing@mit.edu

the outgoing longwave radiation, indicating the existence of high clouds.

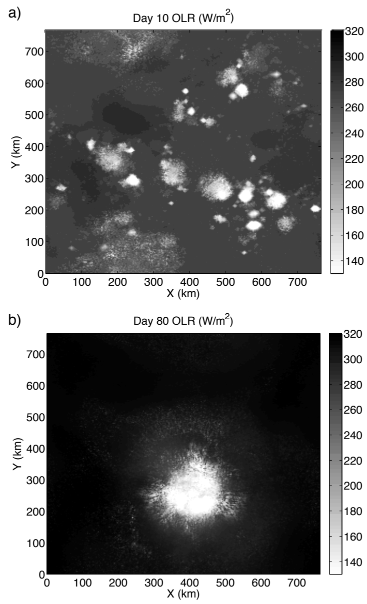

Figure 1: Snapshot of outgoing longwave radiation (OLR) at day 10 (a) and day 80 (b) of a radiative-convective equilibrium simulation at 305 K.

However, when certain conditions are met, the convection becomes organized into a single, intensely convecting moist clump surrounded by a broad region of dry subsiding air, a process termed "self-aggregation" (e.g., Bretherton et al., 2005). In Figure 1b, a snapshot of the outgoing longwave radiation from a later time in the same simulation as Figure 1a, all the clouds are confined to a single cluster. Previous work indicated that cloud-water vapor-radiation feedbacks that dry the drier air columns and moisten the moister air columns are essential to the self-aggregation process (Tompkins and Craig, 1998; Bretherton et al., 2005; Stephens et al., 2008; Muller and Held, 2012).

Simulations at SST's of 301K, 303K , 305K and 307K self-aggregated, while the simulations at lower values of SST did not. We note in passing that the simulations at higher SSTs (i.e., 310 K) need a larger domain to aggregate. Aggregation is characterized by a dramatic increase in the domain averaged outgoing longwave radiation, which coincides with a dramatic decrease in the tropospheric humidity. An examination of the evolution of self-aggregation reveals that it begins as a dry patch that expands, eventually forcing all the convection into a single clump (Wing and Emanuel, 2013). Over the first half of the simulation, the dry regions get progressively drier and larger; it is not until day 50 that the humidity in the moist regions increases. Therefore, when examining the initiation of self-aggregation, we focus on processes that can amplify the initial dry patch.

We perform a sensitivity test at 305 K in which we prescribe the water vapor profile used in the longwave radiation calculation (but still use the modeled clouds) and find that this prevents aggregation. Prescribing the water vapor profile used in the shortwave radiation calculation does not prevent aggregation, indicating it is the longwave radiation - water vapor interaction that is key (in contrast to the results of Muller and Held (2012), who found that the longwave-low cloud interaction was vital). A second sensitivity test in which we use the horizontal mean surface wind speed in the surface enthalpy flux calculation reveals that, at least for the simulation considered here, wind-dependent surface fluxes are necessary for aggregation.

4. ANALYSIS FRAMEWORK

We frame our analysis in terms of the budget for the spatial variance of vertically integrated frozen moist static energy (FMSE). Since column radiative flux conference and surface enthalpy fluxes are diabatic sources and sinks of vertically integrated FMSE, framing our analysis in this matter allows us to quantify these potential feedbacks. The frozen moist static energy, which is conserved during moist adiabatic processes in the model, including the freezing and melting of precipitation, is given by

$$h = c_p T + gz + L_v q_v - L_f q_{ice} \tag{1}$$

where L_f is the latent heat of fusion and q_{ice} represents all ice phase condensates. The budget equation for the spatial variance of vertically integrated frozen moist static energy is given by

$$\begin{aligned} \frac{1}{2}\frac{\partial \hat{h}'^2}{\partial t} &= \hat{h}'\mathsf{SEF}' + \hat{h}'\mathsf{NetSW}' \\ &+ \hat{h}'\mathsf{NetLW}' - \hat{h}'\nabla_h \cdot \widehat{\vec{u}h} \end{aligned} \tag{2}$$

where the primes indicate an anomaly from the horizontal mean. $\hat{h}$ indicates the density weighted vertical integral of FMSE. NetLW and Net SW are the column longwave and shortwave radiative flux convergences, respectively, given by

$$\mathrm{NetLW} = \mathrm{LW_{sfc}} - \mathrm{LW_{top}}, \tag{3}$$

and

$$\mathrm{NetSW} = \mathrm{SW_{top}} - \mathrm{SW_{sfc}}. \tag{4}$$

The surface enthalpy flux anomalies can be written as

$$
\begin{aligned}
\mathrm{SEF}' = &\overbrace{\rho L_v \left(c_E U\right)' \{\Delta q\} + \rho c_p \left(c_H U\right)' \{\Delta T\}}^{\text{(i)}} \\
&+ \overbrace{\rho L_v \{c_E U\} \Delta q' + \rho c_p \{c_H U\} \Delta T'}^{\text{(ii)}} \\
&+ \overbrace{\rho L_v \left(c_E U\right)' \Delta q' + \rho c_p \left(c_H U\right)' \Delta T'}^{\text{(iii)}} \\
&- \overbrace{\rho L_v \{\left(c_E U\right)' \Delta q'\} - \rho c_p \{\left(c_H U\right)' \Delta T'\}}^{\text{(iii)}},
\end{aligned}
\tag{5}
$$

in which $\{A\}$ represents a horizontal mean, A' represents the anomaly from that mean, $\Delta q = q^*_{T_s} - q_v$, and $\Delta T = T_s - T_a$. Term (i) in Equation 5 represents the part of the SEF anomaly due solely to variations in the surface wind speed. Term (ii) represents the part of the SEF anomaly due solely to variations in the air-sea enthalpy disequilibrium. Term (iii) represents the part of the SEF anomaly due to the product of variations in the surface wind speed and variations in the air-sea enthalpy disequilibrium, which we refer to as the “eddy term”. The surface exchange coefficients, c_E and c_H, vary strongly with the surface wind speed but only weakly with the air-sea disequilibrium over the range of values found in the simulations; therefore, we have combined the exchange coefficients with the surface wind speed when calculating horizontal means and anomalies with those means.

Self-aggregation is associated with an increase in the variance of vertically integrated FMSE; therefore, processes that increase $\hat{h}'^2$ favor self-aggregation. It is then clear from Equation 2 that if the correlation between the anomaly of a diabatic term and $\hat{h}'$ is positive, then there is an anomalous source of FMSE in a region of already high FMSE and thus a positive feedback on aggregation. For each of the terms in Equation 2, we take a daily average, and then horizontally average over 48 x 48 km^2 blocks to focus on the mesoscale organization. We then sort the blocks according to their column relative humidity, allowing us to examine how the terms evolve as a function of time and moisture-rank. Finally, we normalize each term by the horizontal mean of FMSE variance, $\{\hat{h}'^2\}$. Because $\hat{h}'^2$ increases with time, normalizing in this manner makes it easier to interpret what is happening in the early stage of aggregation, when both the vertically integrated FMSE anomalies and forcing terms are small.

5. RESULTS

Figure 2a is a hovmuller plot of the sum of the diabatic feedback terms (surface flux and column radiative flux convergence terms in Equation 2). The sum of the diabatic feedbacks is positive during the first twenty days of the simulation and strongest in the driest regions. With time, the positive values propagate toward moister regions, in association with the expanding dry patch. This evolution is consistent with our observation that self-aggregation begins as a dry patch that expands. In the moist regions, positive values persist throughout the simulation. We note that the diabatic terms are a negative feedback in the dry regions from day 30 to 70, but $\hat{h}'^2$ is still increasing in those regions over that time period (not shown). This indicates that the horizontal convergence of the vertically integrated flux of FMSE, calculated as a residual from the rest of the budget, must be playing a role. We find that, in the intermediate stages of aggregation, the convergence of the flux of FMSE by the circulation is important in amplifying vertically integrated FMSE anomalies and promoting self-aggregation (Figure 2b). This is consistent with Bretherton et al. (2005) and Muller and Held (2012), who found that mesoscale circulations intensify the later stages of self-aggregation via an up gradient transfer of moist static energy, and will not be explored further here.

Figure 3a-b reinforces the notion of competition between positive and negative feedbacks, as we see that the correlations of vertically integrated FMSE anomalies with the column radiative flux convergence anomalies are mostly positive during the first 60 days of the simulation (when the cluster is developing), while the correlations with the surface enthalpy flux anomalies are predominantly negative from day 20 to day 60. The total surface flux feedback (Figure 3b) is positive during the first twenty days of the simulation and is largest in the driest regions.

In Figures 3c-f, the feedback terms are further decomposed. First, we examine the surface flux feedback and note that the correlation between vertically integrated FSME anomalies and surface enthalpy flux anomalies due to wind speed anomalies (Figure 3d) is mostly positive. This is the "WISHE" feedback; convective gustiness in the moist, intensely convective regions enhances the surface fluxes there. However, while WISHE is a positive feedback for aggregation in our simulations, it’s primary role is to counteract a strongly negative surface flux feedback due to variations in the air-sea enthalpy disequilibrium. Because the simulations have a fixed, uniform sea surface temperature and the surface en-

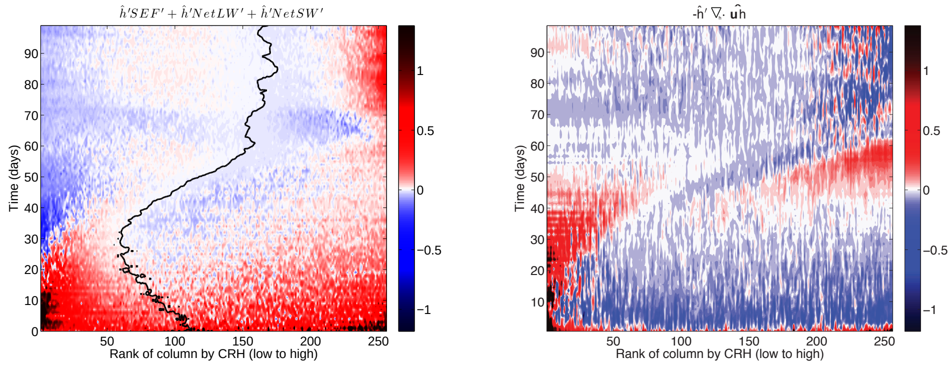

(a) Sum of diabatic terms

(b) Convergence term: $-\hat{h}'\nabla_h \cdot \widehat{\vec{u}h}$

Figure 2: Sum of all diabatic correlation terms (a) and convergence term (b), $-\hat{h}'\nabla_h \cdot \widehat{\vec{u}h}$, (calculated as a residual) in vertically integrated FMSE spatial variance budget, normalized at each time by $\{\hat{h}'^2\}$. Plotted as a function of time (y-axis) and moisture space (x-axis), where each term has been averaged over a day and a 48×48 km^2 block, has units of days^{-1}, and has been sorted according to block-averaged column relative humidity (CRH). On the x-axis, dry regions are on the left and moist regions are on the right. Results are from the simulation at 305 K. The black line is the $\hat{h}'$ = 0 contour. Note that the color bar saturates.

thalpy flux is dominated by the latent heat component, the air-sea enthalpy disequilibrium essentially follows the boundary layer water vapor mixing ratio, which is diminished in the dry columns, enhancing the surface fluxes there (a negative feedback on self-aggregation). Finally, while not shown here, the "eddy term" involving the correlation between vertically integrated FMSE anomalies and the product of wind speed and air-sea disequilibrium anomalies reflects that the wind speed and disequilibrium anomalies are anti-correlated. Summing these components yields a total surface flux feedback that transitions from positive to negative (Figure 3b).

Next, we examine the correlation between the vertically integrated FMSE anomalies and the column shortwave flux convergence anomalies (Figure 3e). This term is positive nearly everywhere, reflecting negative anomalies in NetSW in the dry regions (where $\hat{h}' < 0$) and positive anomalies in NetSW in the moist regions (where $\hat{h}' > 0$). This is due to increasing atmospheric absorption of shortwave radiation by water vapor as we move from dry to moist regions, although this is also modulated by cloud effects (not shown here). In the regions where there are low clouds, the clouds act to increase the column shortwave flux convergence, whereas high clouds in the very moistest regions block solar radiation from penetrating into the lower parts of the atmosphere, decreasing the column shortwave flux convergence.

The feedback term involving column longwave flux convergence anomalies (Figure 3c) is more complicated, as it is can be either positive or negative. Ignoring clouds for the moment, the column longwave flux convergence varies between dry and moist regions because variations in atmospheric water vapor determines variations in the longwave emissivity. Decreasing the water vapor causes competing responses of the longwave radiative fluxes. One effect of decreasing the water vapor in the upper troposphere (as occurs early in the simulation) is that the concentration of longwave emitters will decrease, which locally causes it to radiatively cool less (tending to decrease a sink of energy for the column). However, lower parts of the atmosphere will cool to space more effectively through a more transparent upper troposphere (tending to increase a sink of energy). In the first 20 days, the second effect "wins" and the longwave feedback is initially positive, amplifying the developing dry patch. Later, as the dry perturbation amplifies and the lower troposphere also becomes drier, the longwave feedback transitions from positive to negative because the emissivity has decreased to the extent that the dry regions are no longer able to cool to space effectively (decreasing a sink of energy in the low FMSE regions). A calculation of the longwave feedback term, $\hat{h}'\mathrm{NetLW}'$, using the clear sky longwave fluxes reveals that a large part of the positive longwave feedback at the beginning of the circulation (Figure 3c) is captured by the clear sky processes (Figure 4). Conversely, once the cluster is established (day 60 onward), the longwave feedback is strongly positive in the moistest regions primarily because the column longwave cooling is strongly reduced by the longwave opacity and low temperature

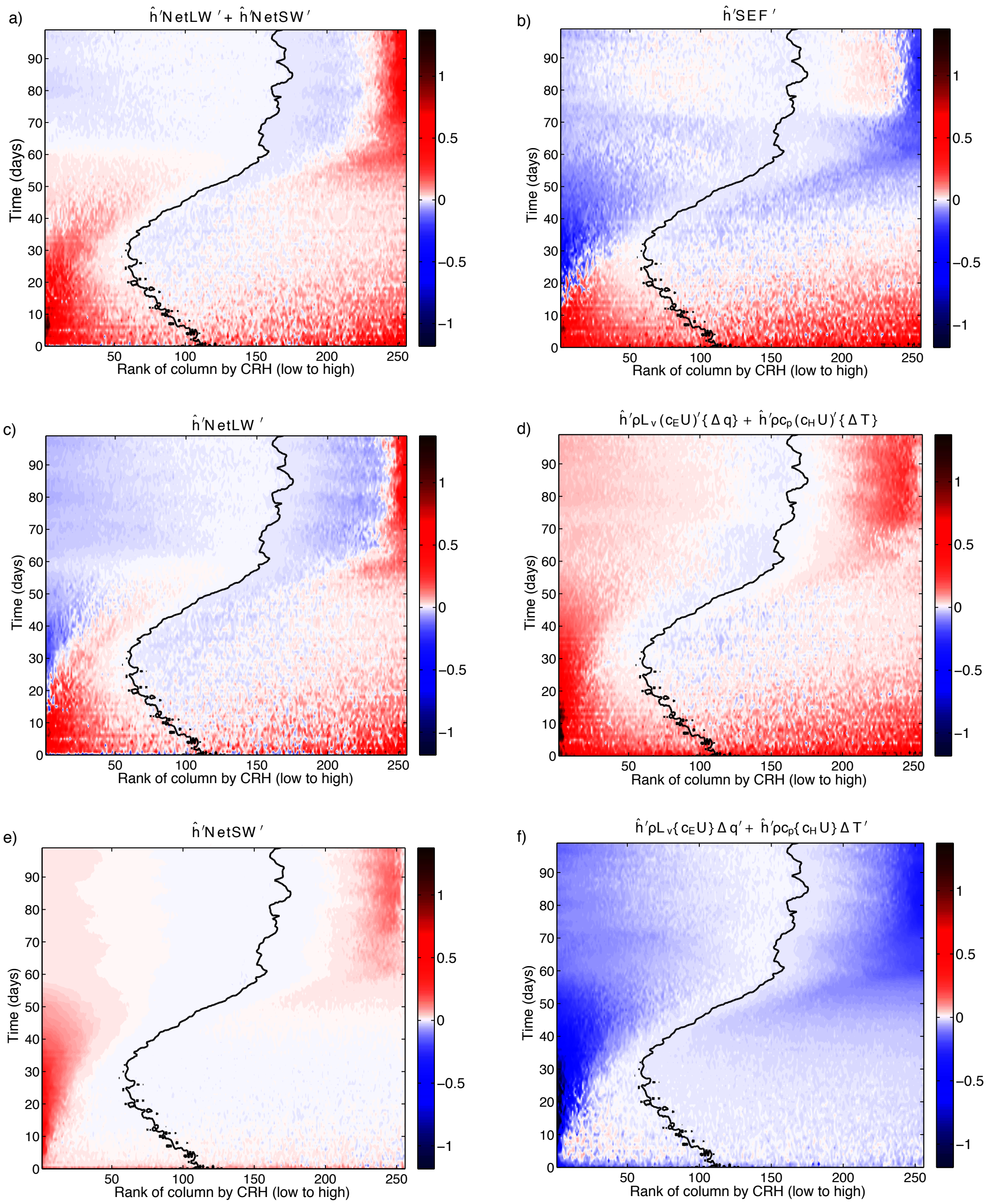

Figure 3: Left column: correlation between vertically integrated FMSE anomalies and column radiative flux convergence anomalies (a: column radiative flux convergence, c: column longwave convergence, e: column shortwave convergence). Right column: correlation between vertically integrated FMSE anomalies and surface enthalpy flux anomalies (b: total surface enthalpy flux anomaly, d: anomaly due to surface wind speed anomalies, f: anomaly due to air-sea enthalpy disequilibrium anomalies). All terms have been averaged over each day and over 48 $\times$ 48 km^2 blocks, normalized by $\{\hat{h}'^2\}$, are from the simulation at 305 K, and have units of days^{-1}. On the x-axis, dry regions are on the left and moist regions are on the right, sorted according to block-averaged column relative humidity (CRH). The black line is the $\hat{h}'$ = 0 contour, plotted as a reference. Note that the color bar saturates in a few places.

of high clouds (compare Figure 4 and Figure 3c).

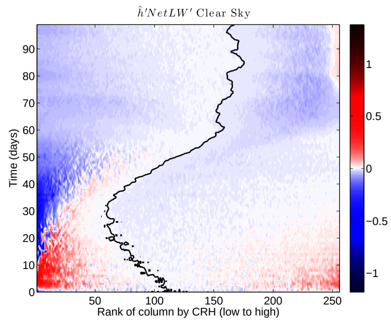

Figure 4: Same as Figure 3c, but for clear sky longwave radiative fluxes.

7. SUMMARY AND IMPLICATIONS FOR TEMPERATURE DEPENDENCE

We introduced a new analysis framework based on the budget for the spatial variance of vertically integrated FMSE, which allowed us to meaningfully quantify each feedback throughout the evolution of self-aggregation. Each of the feedbacks discussed have comparable magnitudes, indicating that each physical mechanism is important for some stage of self-aggregation. Notably, the mechanisms that amplify the initial dry patch and control the evolution to an aggregated state are different from those that maintain the cluster once it is established.

The fact that the longwave - water vapor feedback can be positive or negative depending on the balance of opposing responses to a moisture perturbation suggests it as a candidate for explaining the temperature dependence of aggregation. The results of the sensitivity test in which a prescribed water vapor profile is used in the radiation calculation also point to longwave radiation, rather than shortwave. A companion study, Emanuel et al. (2013), included the longwave - water vapor feedback discussed here in a simple two-layer model (which also included a representation of convection and large-scale vertical velocity), and showed that the model becomes unstable at high temperatures. The instability results because, at high temperature, the emissivity of the lower troposphere is large enough (due to high water vapor concentration) that variations of its radiative cooling depend primarily on variations in upper tropospheric water vapor.

8. ACKNOWLEDGEMENTS

We thank Marat Khairoutdinov for providing SAM, the cloud resolving model. We also acknowledge high-performance computing support from Bluefire and Yellowstone (ark:/85065/d7wd3xhc) provided by NCAR's Computational and Information Systems Laboratory, sponsored by the National Science Foundation. This work was supported by NSF grants 1032244, 1136480, 0850639. The first author received additional support from the MIT Joint Program on the Science and Policy of Global Change. Much of this work was published as part of Wing and Emanuel (2013) and is adapted here in accordance with the Creative Commons Attribution License.

9. REFERENCES

Bretherton, C. S., P. N. Blossey, and M. Khairoutdinov, 2005: An energy-balance analysis of deep convective self-aggregation above uniform SST. *J. Atmos. Sci.*, **62**, 4237–4292.

Emanuel, K., A. A. Wing, and E. M. Vincent, 2013: Radiative-convective instability. *J. Adv. Model. Earth Syst.*, **5**, doi:10.1002/2013MS000 270.

Hennon, C. C., C. N. Helms, K. R. Knapp, and A. R. Bowen, 2011: An objective algorithm for detecting and tracking tropical cloud clusters: Implications for tropical cycloge prediction. *J. Atmos. Oceanic Technol.*, **28**, 1007–1018.

Khairoutdinov, M. F. and D. A. Randall, 2003: Cloud resolving modeling of the ARM summer 1997 IOP: Model formulation, results, uncertainties, and sensitivities. *J. Atmos. Sci.*, **60**, 607–625.

Machado, L. A. T. and W. B. Rossow, 1993: Structural characteristics and radiative properties of tropical cloud clusters. *Monthly Weather Review*, **121**, 3234–3260.

Mapes, B. E. and R. A. Houze Jr., 1993: Cloud clusters and superclusters over the oceanic warm pool. *Monthly Weather Review*, **121**, 1398–1415.

Muller, C. J. and I. M. Held, 2012: Detailed investigation of the self-aggregation of convection in cloud resovling simulations. *J. Atmos. Sci.*, **69**, 2551–2565.

Nesbitt, S. W., E. J. Zipser, and D. J. Cecil, 2000: A census of precipitation features in the tropics using TRMM: Radar, ice scattering, and lightning observations. *J. Climate*, **13**, 4087–4106.

Stephens, G. L., S. van den Heever, and L. Pakula, 2008: Radiative-convective feedbacks in idealized states of radiative-convective equilibrium. *J. Atmos. Sci.*, **65**, 3899–3916.

Tobin, I., S. Bony, C. E. Holloway, J. Y. Grandpeix, G. Seze, D. Coppin, S. J. Woolnough, and R. Roca, 2013: Does convective aggregation need to be represented in cumulus parameterizations? *J. Adv. Model. Earth Syst.*, **5**, doi:/10.1002/jame.20 047.

Tobin, I., S. Bony, and R. Roca, 2012: Observational evidence for relationships between the degree of aggregation of deep convection, water vapor, surface fluxes, and radiation. *J. Climate*, **25**, 6885–6904.

Tompkins, A. and G. Craig, 1998: Radiative-convective equilibrium in a three-dimensional cloud-ensemble model. *Q. J. R. Meteorol. Soc.*, **124**, 2073–2097.

Wing, A. A. and K. A. Emanuel, 2013: Physical mechanisms controlling self-aggregation of convection in idealized numerical modeling simulations. *J. Adv. Model. Earth Syst.*, **5**, doi:10.1002/2013MS000 269.